

Quasistatic electric-field-modulated optical pattern transition in a thin nematic liquid-crystal film with a single feedback mirror

Hsu-Kuan Hsu, Yinchieh Lai, and Shu-Hsia Chen

Citation: [Applied Physics Letters](#) **85**, 2724 (2004); doi: 10.1063/1.1795363

View online: <http://dx.doi.org/10.1063/1.1795363>

View Table of Contents: <http://scitation.aip.org/content/aip/journal/apl/85/14?ver=pdfcov>

Published by the [AIP Publishing](#)

Articles you may be interested in

[Submillisecond response nematic liquid crystal modulators using dual fringe field switching in a vertically aligned cell](#)

Appl. Phys. Lett. **92**, 111101 (2008); 10.1063/1.2896650

[Electro-optic modulation using single-crystal film of an organic molecular salt in a Fabry-Perot cavity](#)

Appl. Phys. Lett. **87**, 191111 (2005); 10.1063/1.2130394

[In-fiber nematic liquid crystal optical modulator based on in-plane switching with microsecond response time](#)

Appl. Phys. Lett. **81**, 5243 (2002); 10.1063/1.1532532

[Frequency modulation response of a liquid-crystal electro-optic device doped with nanoparticles](#)

Appl. Phys. Lett. **81**, 2845 (2002); 10.1063/1.1511282

[Interdependence of the electrical and optical properties of liquid crystals for phase modulation applications](#)

J. Appl. Phys. **87**, 4069 (2000); 10.1063/1.373032

The advertisement features a dark blue background with white and orange text. At the top left, it reads 'NEW! Asylum Research MFP-3D Infinity™ AFM' in large white letters, followed by 'Unmatched Performance, Versatility and Support' in orange. On the right, the Oxford Instruments logo is shown with the tagline 'The Business of Science®'. Below the text are four images: a textured surface, a circular pattern, a grid of small squares, and the AFM instrument itself. Each image is accompanied by a short text description: 'Stunning high performance', 'Simpler than ever to GetStarted™', 'Comprehensive tools for nanomechanics', and 'Widest range of accessories for materials science and bioscience'.

Quasistatic electric-field-modulated optical pattern transition in a thin nematic liquid-crystal film with a single feedback mirror

Hsu-Kuan Hsu,^{a)} Yinchieh Lai, and Shu-Hsia Chen

Institute of Electro-Optical Engineering, National Chiao Tung University, 1001 Ta Hsueh Road, Hsinchu 300, Taiwan, Republic of China

(Received 30 October 2003; accepted 19 July 2004)

We present here the pattern formation in the transverse profile of a continuous-wave laser beam passing through a parallel planar-aligned nematic liquid crystal (NLC) film biased by a quasistatic electric field and then reflected back to the sample cell by a single planar mirror. The effect of the biasing voltage is studied through the ability to change the nonlinearity by modulating the orientation of the NLC molecules electrically. By suitably modulating the quasistatic electric field the optical pattern transition from the hexagon to the roll is achieved. The pattern transition can be explained by the linear stability analysis for the nonlinear liquid crystal film with optical feedback. © 2004 American Institute of Physics. [DOI: 10.1063/1.1795363]

As is proposed and demonstrated by Firth and D'Allessandro, a simple optical system for optical pattern formation is constituted by placing a thin Kerr medium in front of a planar feedback mirror.^{1,2} For these systems the spontaneously generated patterns will typically form as hexagons. By breaking the rotational symmetry or using a spatial filter one can observe patterns other than hexagons.³⁻⁶ If the nematic liquid crystal (NLC) films are used as the nonlinear media, three kinds of operating modes have been used to observe the transverse pattern formation.⁷⁻⁹ Nevertheless, a quasistatic electric field biased parallel planar-aligned NLC film has not been used to observe the transverse pattern formation. Recently, we succeed in observing optical pattern formation by using such NLC films. The anisotropic distribution of the threshold intensity for the patterns to be formed makes the optical patterns can be switched between the roll and the hexagon by controlling the input light power.¹⁰ However, the effect of the biasing voltage in this one-feedback-mirror system has not been studied. From our previous works we know that the optical nonlinearity for such NLC films can be effectively modulated by suitably applying a quasistatic electric field.^{11,12} This is due to the unique properties of liquid crystal films. A nematic liquid crystal film can not only be an anisotropic film but also an inhomogeneous optical film. In particular, these optical properties can be modulated electrically utilizing its dielectric anisotropy. For example, consider the liquid crystal with positive dielectric anisotropy, the director tends to be parallel with the applied electric field via the effects of the induced electric dipole. In this letter, we present the analysis of the effect of the biasing voltage through the ability of changing the nonlinearity by electrically modulating the orientation of the NLC molecules, which effectively modulates its optical anisotropy and threshold distribution. Considering both the anisotropic property of the threshold intensity for the pattern formation and the effect of the biasing voltage a simple electric method to obtain the roll and the hexagon at single input light power is successfully achieved. The experimental results reasonably agree with that predicted by the theoretical linear stability

analysis for the nonlinear liquid crystal film with optical feedback.

The work in this paper looks similar with that in Ref. 10. However, in this letter not only the intrinsic elastic anisotropy of the liquid crystals is considered but also the key topic of the effect of the biasing voltage is studied. The consideration of both the elastic and dielectric anisotropies can give further extensive understanding and applications in the optical pattern formation phenomena. Not only the experimental operating becomes easier but also the mechanism for the pattern-formation phenomena by using the electric-field biased NLC film is clearer.

Following the one-feedback-mirror system, the coordinates and the derivations in Ref. 10 the general diffusion-like equation for the optically induced optical phase variation in the transverse plane can be expressed as

$$\tau \frac{\partial \psi}{\partial t} - l_x^2 \left(\frac{\partial^2 \psi}{\partial x^2} \right) - l_y^2 \left(\frac{\partial^2 \psi}{\partial y^2} \right) + \psi = \alpha I, \quad (1)$$

where ψ is the optically induced phase variation, τ is the response time, I is the input intensity, l_i ($i=x, y$) is the diffusive length in the i direction and α is the effective nonlinear coefficient. Then the threshold intensity for the optical pattern formation can be easily obtained by the linear stability analysis (LSA) of Eq. (1) which assuming that a small sinusoidal phase modulation is applied to the forward plane wave and can be expressed as

$$I_{th}(q, \varphi) = \frac{1 + q^2(l_x^2 \cos^2 \varphi + l_y^2 \sin^2 \varphi)}{2R\alpha \sin\left(\frac{q^2}{2\pi} \lambda_0 L\right)}, \quad (2)$$

where q is the wave-vector of the perturbation, φ is the azimuthal angle starting from the x axis clockwise, λ_0 is the optical wavelength in vacuum, R is the reflectivity of the reflecting mirror, and L is the length between the sample and

^{a)}Electronic mail: hkhsu.eo87g@nctu.edu.tw

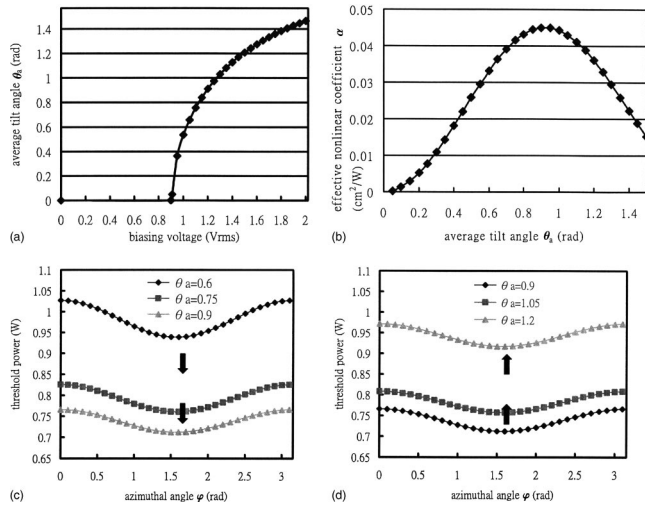


FIG. 1. (a) Calculated average tilt angle θ_a vs the biasing voltage; (b) effective nonlinear coefficient α vs the average tilt angle θ_a ; (c) calculated threshold power distribution for different θ_a ; from the top to the bottom are $\theta_a = 0.6, 0.75$, and 0.9 rad, respectively. (d) Calculated threshold power distribution for different θ_a ; from the bottom to the top are $\theta_a = 0.9, 1.05$, and 1.2 rad, respectively; with beam diameter = 1.4 mm, $d = 68 \mu\text{m}$, $L = 1.9$ cm, $R = 0.65$, input light power = 0.91 W.

the reflecting mirror. The coefficient in Eqs. (1) and (2) can be expressed as

$$l_x^2 = \frac{1}{G} \left(\frac{d}{\pi} \right)^2 \left[1 + \frac{k}{2} \left(1 + 2J_0(2\theta_a) - \frac{J_1(2\theta_a)}{\theta_a} \right) \right]; \quad (3)$$

$$l_y^2 = \frac{1}{G} \left(\frac{d}{\pi} \right)^2 \left(\frac{k_{22}}{k_{11}} \right); \quad \alpha = - \frac{2\pi n_e \mu d J_1(2\theta_a)^2}{\lambda_0 I_{fr} G},$$

where

$$G = \left[2 + k \left(1 - \frac{J_0(2\theta_a)}{2} + \frac{J_2(2\theta_a)}{2} \right) \right]; \quad (4)$$

$$I_{fr} = ck_{11} \frac{\left(\frac{\pi}{d} \right)^2}{(-n_e \mu)}; \quad V_{th} = 2\pi \left(\frac{\pi k_{11}}{\epsilon_{\parallel} - \epsilon_{\perp}} \right)^{1/2},$$

where θ_a is the electrically biased average tilt angle of the liquid crystal directors in the middle layer of the liquid crystal cell, $k = (k_{33}) / (k_{11}) - 1$, $\mu = 1 - (n_e)^2 / (n_o)^2$, k_{11} , k_{22} and k_{33} are the splay, twist, and bend elastic constants, c is the velocity of light in vacuum, d is the thickness of the liquid crystal cell, I_{fr} and V_{th} are Freedericksz optical intensity and voltage. Furthermore, n_e and n_o , ϵ_{\parallel} and ϵ_{\perp} are the refractive indices and the dielectric constants with their directions parallel and perpendicular to the liquid crystal director, respectively. The tilt angle θ_a depends on the applied voltage and the input optical intensity. For a fixed input intensity, θ_a is tunable by the applied voltage. In other words, the anisotropies of the diffusion lengths and the threshold intensity are tunable by the applied voltage as well.

Considering the using of the positive-dielectric-anisotropic NLC materials the orientation of the liquid crystal director tends to be parallel with the direction of the applied electric field and the average tilt angle θ_a can be obtained by minimizing the total free energy under the hard

boundary and a uniformly distributed electric field assumptions. By following the Euler-Lagrange optimization process θ_a has to obey the equation expressed as:

$$\theta_a \left(2 + \frac{k}{2} [2 - J_0(2\theta_a) + J_2(2\theta_a)] \right) = \left(\frac{V^2}{V_{th}^2} - \frac{I}{I_{th}} + \frac{k}{4} \right) 2J_1(2\theta_a). \quad (5)$$

The above equation can be calculated numerically if d , V , I , and the material parameters are known. Furthermore, θ_a is dominated by the electric field for weak input power. From Eq. (2), the threshold intensity as a function of q is expected to reach its minimum approximately when $\sin[(q^2 \lambda_0 L) / (2\pi)] = 1$ or equivalently when $q \cong \pi / \sqrt{\lambda_0 L}$.

From Eqs. (2) and (3), one can see that the diffusion lengths in x and y directions are anisotropic. As we explained in Ref. 10, this property results in the anisotropic distribution of the threshold intensity for the patterns to be formed. Besides the intrinsic elastic anisotropic property, the biasing voltage indeed plays an important role in the optical pattern formation phenomena once a quasistatic electric field biased parallel planar-aligned NLC film is used. Since the positive-dielectric-anisotropic NLC films are used the orientation of the liquid crystal directors is changed when the applied voltage exceeds the Freedericksz voltage V_{th} (in our case $V_{th} = 0.9 V_{rms}$). As an example, from Eq. (5) we plot the changing of θ_a with respect to the applied biasing voltage and is shown in Fig. 1(a). From Eqs. (3) and (4), the changing of θ_a affects the diffusion lengths. Furthermore, from Eqs. (2)–(4), not only the diffusion lengths but also the effective nonlinear coefficient α will be changed when θ_a is changed. From Fig. 1(a), we can see that θ_a can be modulated by the applied biasing voltage. Therefore, we plot α with respect to θ_a as shown in Fig. 1(b). From Fig. 1(b), we see that α initially increases with θ_a increasing and reaches a maximum when θ_a is about 0.9 rad. However, when θ_a is larger than 0.9 rad α decreases with θ_a increasing. Furthermore, the changing behavior of α with respect to θ_a directly affects the threshold intensity distribution when θ_a is changed. Figures 1(c) and 1(d) show the theoretical threshold power at different θ_a for convenient. The threshold power is obtained by the product of Eq. (2) and the beam area. In our calculation the beam diameter is assumed to be 1.4 mm. From Figs. 1(c) and 1(d), the threshold power distribution decreases with θ_a increasing when θ_a is smaller than 0.9 rad and increases with θ_a increasing when θ_a is larger than 0.9 rad. Therefore, considering both the anisotropic distribution of the threshold power and the electric-modulated property of the effective nonlinear coefficient α an electric method to obtain different optical patterns can be expected. When θ_a is initially biased at a value smaller than 0.9 rad, one can input a suitable light power larger than the maximum threshold (in our case the maximum locates at $\varphi = 0^\circ$ and 180°) and the hexagon is expected to be obtained on the basis of its compact structure. This is similar to that in the isotropic case and we can expect the oscillation of three ripple patterns leading to hexagons formation.¹³ Decreasing the biasing voltage which decreasing θ_a results in the increasing of the threshold. Once the minimum threshold (in our case the minimum locates at $\varphi = 90^\circ$) for a value of θ_a is smaller and close to the input light power only the mode with the lowest threshold power will be enhanced and the roll pattern should be observed. On the

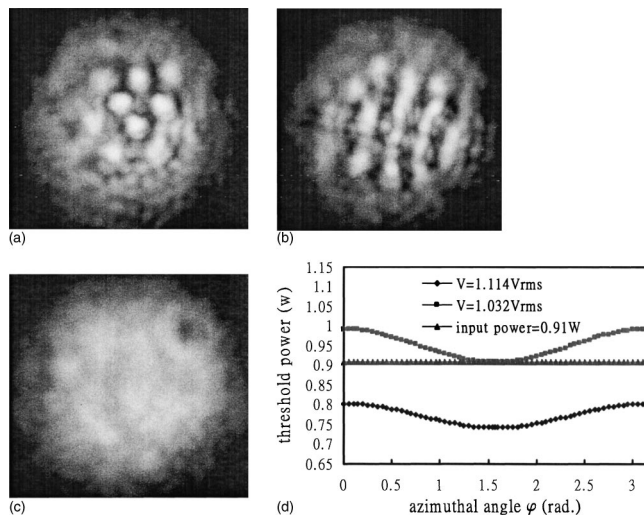


FIG. 2. Near-field images of the reflected beam at the cell showing the transition from the hexagon to the roll: (a) Biasing voltage = 1.114 V_{rms} ; (b) biasing voltage = 1.032 V_{rms} ; (c) biasing voltage = 0 V_{rms} ; (d) calculated threshold power vs the azimuthal angle φ , from the bottom to the top are biasing voltage = 1.114 and 1.032 V_{rms} , respectively. The horizontal line indicates the input light power = 0.91 W; with beam diameter = 1.4 mm, $d = 68 \mu\text{m}$, $L = 1.9 \text{ cm}$, $R = 0.65$.

other hand, if the hexagons are observed when θ_a is initially biased larger than 0.9 rad one has to increase the biasing voltage to see the roll pattern.

In our experiment, the setup arrangement is the same as in Ref. 10 and the sample cell is a nematic liquid-crystal (E7) film sandwiched between two indium-tin-oxide coated glass windows. We use polyvinyl alcohol (PVA) as the alignment material and achieve the parallel planar alignment by rubbing. The applied external fields, include a 1 kHz electric field generated by a microcomputer's waveform synthesizer (Quatech Inc., WSB-A12M) and the p -polarized optical field at the wavelength of 514.5 nm from an Ar-ion laser. The original beam waist from the Ar-ion laser is 1.9 mm and the input beam diameter is controlled by the pinhole as 1.4 mm. We use the pinhole to block the stray light in the low intensity wings of the beam and let the high intensity region pass through the sample. The reflectivity of our reflecting mirror is about 0.65. With the cell gap of 68 μm , the feedback length of 1.9 cm, and the input light power of 0.91 W, the curve of the threshold power for different azimuthal angles can be calculated by the product of Eq. (2) and the beam area and the results are shown in Fig. 2(d). Though the actual laser beam is a Gaussian beam, for simplicity, we calculate the threshold power from the threshold intensity multiplied by the beam area since only the light with high intensity passing through the pinhole and the sample. The threshold power with the peak intensity reaching the threshold intensity should be lower than that shown in Fig. 2(d). The input light power has been indicated in Fig. 2(d) as a horizontal line to compare with the theoretical threshold power curves and it is measured after the beam passing through the pinhole and the beam splitter. In our experiments, the laser beam is

blocked when we change the biasing voltage. Therefore, the pattern formations are always starting from the homogeneous state. The images of the observed near-field patterns are shown in Figs. 2(a) and 2(b) and the transition from the hexagon to the roll can be clearly seen. Figure 2(c) shows the picture when the biased voltage is zero and there is no pattern formed. This is because the liquid crystal directors will not be rotated when the applied voltage is below the Freedericksz voltage V_{th} .

In our calculation, we set the spatial frequency q as $q \cong (\pi)/(\sqrt{\lambda_0 L})$. The accuracy of such an approximation has been verified by measuring the relations between the feedback length and the pattern period. The pattern period for the feedback length $L = 1.9 \text{ cm}$ is 198 μm and the theoretically predicted value is 197.74 μm . The experimental results agree with the theoretical predictions reasonably well.

In conclusion, we have observed interesting spontaneous pattern formation by using a quasistatic electric field biased parallel planar-aligned NLC film with a single feedback mirror. The intrinsic anisotropy of the threshold intensity distribution makes the switching of the formed patterns possible. Since the effective nonlinear coefficient can be modulated by controlling the average tilt angle θ_a electrically, the optical pattern transition between the hexagon and the roll can be easily achieved by suitably modulating θ_a by the biasing voltage even for a single input laser power. The observed phenomena can be reasonably explained by the results from the linear stability analysis of the governing diffusion-like equation.

The consideration of both the elastic and dielectric anisotropies can give further extensive understanding and applications in the optical pattern formation phenomena. Not only the experimental operating becomes easier but also the mechanism for the pattern-formation phenomena by using the electric-field biased NLC film is clearer.

This work was partially supported by the National Science Council, R.O.C., under Contract No. NSC 92-2112-M-009-025.

¹W. J. Firth, *J. Mod. Opt.* **37**, 151 (1990).

²G. D'Allessandro and W. J. Firth, *Phys. Rev. Lett.* **66**, 2597 (1991).

³E. Ciarabella, M. Tamburrini, and E. Santamato, *Appl. Phys. Lett.* **64**, 3080 (1994).

⁴G. Agez, C. Szwarz, E. Louvergneaux, and P. Glorieux, *Phys. Rev. A* **66**, 063805 (2002).

⁵E. Benkler, M. Kreuzer, R. Neubecker, and T. Tschudi, *Phys. Rev. Lett.* **84**, 879 (2000).

⁶B. Gütlich, R. Neubecker, M. Kreuzer, and T. Tschudi, *Chaos* **13**, 239 (2003).

⁷R. Macdonald and H. J. Eichler, *Opt. Commun.* **89**, 289 (1992).

⁸M. Tamburrini, M. Bonavita, S. Wabnitz, and E. Santamato, *Opt. Lett.* **18**, 855 (1993).

⁹R. Neubecker, G.-L. Oppo, B. Thuring, and T. Tschudi, *Phys. Rev. A* **52**, 791 (1995).

¹⁰H.-K. Hsu, S.-H. Chen, and Y. Lai, *Opt. Express* **12**, 1320 (2004).

¹¹S.-H. Chen, J. Y. Fan, and J.-J. Wu, *J. Appl. Phys.* **83**, 1337 (1998).

¹²Y. Shen, H.-K. Hsu, and S.-H. Chen, *J. Opt. Soc. Am. B* **20**, 65 (2003).

¹³G. D'Allessandro and W. J. Firth, *Phys. Rev. A* **46**, 537 (1992).